NRL Report 6580

Calculations of Stellar Structure

CARL A. ROUSE

E. O. Hulburt Center for Space Research

and

University of California
Space Sciences Laboratory
Berkeley, California

September 18, 1967

APPROVED FOR PUBLIC
RELEASE - DISTRIBUTION
UNLIMITED

NAVAL RESEARCH LABORATORY
Washington, D.C.

This page intentionally left blank.

CONTENTS

Preface	iv
Problem Status	iv
Authorization	iv
INTRODUCTION	1
BASIC EQUATIONS	1
PHYSICAL INPUT	3
Equation of State	3
Adiabatic Changes in an Ionizing Gas	3
Opacity	8
Energy Generation	9
RESULTS	9
DISCUSSION	12
Stability Conditions Derived From Real-Gas Properties	15
Mass – Central Density Relationship	17
Results With Improved Programs	18
SUMMARY AND CONCLUSIONS	21
ACKNOWLEDGMENTS	21
REFERENCES	22

PREFACE

Calculations of the author's solar model, reported at the New York APS meeting, Jan. 1965, were continued at the Naval Research Laboratory as part of a research program undertaken as an E. O. Hulburt Research Appointee. Of particular significance is that due to the increased mathematical and physical accuracies introduced at NRL, the resulting photospheric densities lead to mean atomic volumes in excellent agreement with those needed to explain the drop in intensity of photospheric hydrogen lines through screening. The solar model itself is the first known continuous calculation — from the center through the photosphere — of the sun's mass, radius, and luminosity. The resulting model, incidentally, yields values of electron pressure and temperature in the photosphere in good agreement with the currently accepted photospheric values.

The present report reviews the method and the progress leading to the present equilibrium model with the inclusion of results obtained as part of current NRL research. This review is to be published in Vol. 2 of "Progress in High Temperature Physics and Chemistry," of which the author is the editor for Pergamon Press.

PROBLEM STATUS

This is a survey report of work accomplished on the problem; work on these and other phases of the problem is continuing.

AUTHORIZATION

NRL Problem A01-02
Project RR 004-02-42-5300
Sponsored jointly by the Office of Naval Research
and the National Science Foundation

Manuscript submitted April 19, 1967.

CALCULATIONS OF STELLAR STRUCTURE

INTRODUCTION

This report will review a method of calculating stellar structure — with consideration of the structure of the sun only — based upon a real-gas equation of state that describes a mixture of monatomic gases in ionization equilibrium. The investigation was undertaken to determine whether or not calculations of the structure of the sun could be improved by using a real-gas equation of state and if the calculated structure might be sensitive to aspects of the equation of state. A review of the literature indicated that some limitations of previous calculations of stellar structure are (a) the assumption of a constant γ-law perfect-gas equation of state, (b) the assumption of a constant mean molecular weight μ or of a μ that is only a function of the relative abundance, (c) the assumption that the electron density is proportional to the mass density in Kramer's opacity formula, (d) that the method of calculating the profile leads to zero or negative temperatures near the star boundary — for the sun, this has usually been considerably short of the radius, and (e) that because of (d) a massless, perfect-gas envelope is assumed and tacked on to the aborted solution to account for the known radius.

With the derivation of an ionization equilibrium equation of state (IEEOS) for a mixture (1-3) it was immediately recognized that the stellar envelope calculations could surely be improved. Hence, stellar profile calculations were begun wherein the above restrictions were relaxed through the use of the IEEOS. The basic objectives of the investigation were to calculate the mass, radius, and luminosity of the sun and then to compare the results when variations were introduced into the IEEOS. The general approach was to assume a central temperature T_c and central density ρ_c and to calculate outward to the photosphere, stopping the calculations when $T_f \lessapprox 0.5$ eV (5800°K). Because of uncertainties in the energy generation cycles — including the relative abundances of the elements in the central region — the solar mass and solar radius at $T = T_f$ were the basic quantities sought.

For more general discussions of the analysis of stellar structure, the reader is referred to texts by Chandrasekhar (4), Kuiper (5), Schwarzschild (6), Aller and McLaughlin (7), and Motz and Duveen (8). The particular reports of interest are those by the author (9). The text by Schwarzschild was found to be the most useful.

BASIC EQUATIONS

The basic equations describing hydrostatic equilibrium, thermal equilibrium, and energy transport are given as

$$\frac{dP}{dr} = -\rho\frac{GM_r}{r^2} , \tag{1}$$

$$\frac{dM_r}{dr} = 4\pi r^2\rho , \tag{2}$$

$$\frac{dL_r}{dr} = 4\pi r^2\rho\epsilon , \tag{3}$$

$$\frac{dT}{dr} = -\frac{3}{4ac}\frac{K\rho}{T^3}\frac{L_r}{4\pi r^2} \text{ (radiative)}, \tag{4}$$

or

$$\frac{dT}{dr} = \frac{\gamma - 1}{\gamma}\frac{T}{P}\frac{dP}{dr} \text{ (convective)}, \tag{5}$$

where the symbols have the standard meanings (6). With electronic computers available the straightforward approach is a finite differencing scheme, or the linear term of a Taylor expansion. The difference equivalents for the above system of equations become

$$P_{j+1} = P_j + \left(\frac{dP}{dr}\right)_j \Delta r_j , \tag{6}$$

$$T_{j+1} = T_j + \left(\frac{dT}{dr}\right)_j \Delta r_j , \tag{7}$$

$$\rho_{j+1} \longleftrightarrow \text{IEEOS}(P_{j+1}, T_{j+1}) , \tag{8}$$

$$M_{j+1} = M_j + \left(\frac{dM_r}{dr}\right)_{j+1/2} \Delta r_j , \tag{9}$$

$$L_{j+1} = L_j + \left(\frac{dL_r}{dr}\right)_{j+1/2} \Delta r_j , \tag{10}$$

$$r_{j+1} = r_j + \Delta r_j , \tag{11}$$

and

$$\Delta r_j = \Delta R_\odot / 2^n , \tag{12}$$

where the index j denotes the finite zone boundary with $j = 0$ at the center. For small initial Δr the above quantities at $j = 1$ $(r = \Delta r)$ are calculated using central values (6). The index $j + 1/2$ denotes the mean value of j and $j + 1$. The values of n in Eq. (12) are 0, 1, 2, . . . , as explained below.

In the solution the pressure P and temperature T are advanced using Eqs. (6) and (7). In Eq. (7) the minimum temperature gradient from Eq. (4) or (5) is used. With P_{j+1} and T_{j+1} the IEEOS is used to determine ρ_{j+1}. But the IEEOS takes ρ and T as inputs; hence the density is iterated until a pressure is calculated that is within a given relative difference of P_{j+1}. The corresponding density is taken as ρ_{j+1}. Next, the opacity, energy generation, mass, and luminosity at $j + 1$ are computed.

Linearity is assured by controlling Δr. Define $\Delta P_j = |P_{j+1} - P_j|$ and $\Delta T_j = |T_{j+1} - T_j|$. Now, at each zone, test $\Delta T_j/T_j$ and $\Delta P_j/P_j$ against a given δ and demand that <u>both</u> be equal to or less than the given δ, or

$$\Delta T_j/T_j \leqq \delta \quad \text{and} \quad \Delta P_j/P_j \leqq \delta . \tag{13}$$

If either is greater than δ, Δr is reduced by a factor of 2, and then both T_{j+1} and P_{j+1} are recalculated. Hence, the actual Δr_j used is given by Eq. (12). Values of $\Delta R_\odot$ (where $\odot$ indicates the sun) used are 10^{-3} $R_\odot$ or less, with Δr becoming as low as 10^{-5} $R_\odot$ near the photosphere.

The above method is essentially that used by Chandrasekhar (4) in his proof of the Vogt-Russell theorem.

PHYSICAL INPUT

Equation of State

The equation of state used is the mixture ionization equilibrium equation of state (IEEOS) derived by the author, with the high-density formulation also developed by the author (1-3, 9-13). The relative abundances assumed for the elements will be those of Goldberg, Müller, and Aller (14) with the helium abundance being left as a parameter in order to vary the mean molecular weight μ. For computational speed, only the five most abundant elements were used in the calculations, with the helium relative number abundance given by

$$He = D_o \left\{1.0 + D_1 \exp\left[- D_2 (M_r/M_\odot)^{D_3}\right]\right\} , \tag{14}$$

where D_o, D_1, D_2, and D_3 are arbitrary input constants. The expression given in Eq. (14) is not arbitrary. This relationship is a generalization of the helium variation derived by Schwarzschild (6a). Since the use of published magnitudes did not lead to mass and radius agreement, the central helium abundance and its variation were left as parameters $_\odot$ in the basic theoretical problem of a continuous calculation of $M_\odot$, $R_\odot$, and $L_\odot$.

The approximate analytical partition functions used initially were those derived by Fowler for a single excited electron and referred to as the Planck or Urey-Fermi partition functions (15).

With the use of either of these partition functions, one can easily derive an approximate expression for the energy in highly excited states. With Fowler's assumption that the energies of the levels are near the ionization energy $I^{i,j}$ the approximate excitation energy becomes

$$E_x = \sum_j \sum_i \frac{\sum_s E_s^{i,j} g_s^{i,j} \exp(-E_s^{i,j}/kT)}{\sum_s g_s^{i,j} \exp(-E_s^{i,j}/kT)} \tag{15}$$

and

$$E_x \approx \sum_j \sum_i \left[I^{i,j}(u^{i,j} - g_1^{i,j})\right]/u^{i,j} ,$$

where $u^{i,j}$ is either of Fowler's approximate expressions and $g_1^{i,j}$ is the corresponding ground state degeneracy. The indexes refer to electronic state s of ion i of element j. The total internal energy becomes

$$E = \frac{3}{2}P + E_{ionization} + E_{excitation} , \tag{16}$$

and an effective gamma will be defined by $\gamma_e - 1 = P/E$. The effective gamma γ_e is to be distinguished from the constant $\gamma = 5/3$.

For other calculations of γ_e see the report by Hilsenrath, Green, and Beckett (16).

Adiabatic Changes in an Ionizing Gas

Consider a substance with γ_e defined as above by

$$\gamma_e - 1 = P/E \,, \tag{17}$$

where P and E are the pressure and internal energy per unit volume, respectively. (The exact equations for the pressure and internal energy are left unspecified.) In a reversible adiabatic change $dQ = 0$ or

$$dE_g - \frac{P}{\rho^2}\, d\rho = 0 \,, \tag{18}$$

where $E_g = E/\rho$, the internal energy per unit mass. From Eq. (17)

$$E_g = P/\rho(\gamma_e - 1) \,. \tag{19}$$

Substituting Eq. (19) into Eq. (18) yields

$$\frac{dP}{P} = \gamma_e \frac{d\rho}{\rho} + \frac{d(\gamma_e - 1)}{\gamma_e - 1} \,. \tag{20}$$

Unless $\gamma_e(\rho, T)$ is known, Eq. (20) cannot be integrated. However, for small changes in ρ about ρ_o and in T about T_o, $\gamma_e(\rho, T) \approx \text{constant} = \gamma_e(\rho_o, T_o)$, or

$$P \approx B\rho^{\gamma_e(\rho_o, T_o)} \tag{21}$$

with B a constant. Another approximate solution to Eq. (20) is obtained if one neglects changes in γ_e in the coefficient of $d\rho/\rho$ only, yielding

$$P \approx B'(\gamma_e - 1)\rho^{\gamma_e(\rho_o, T_o)} \tag{22}$$

where $|\gamma_e - \gamma_e(\rho_o, T_o)|$ is small. If one approximates the pressure along the equilibrium profile with Eq. (22), allowing both γ_e's to vary, then

$$\frac{d\rho}{dr} \approx \frac{\rho}{\gamma_e P}\frac{dP}{dr} - \frac{\rho}{\gamma_e(\gamma_e - 1)}\left[1 + (\gamma_e - 1)\ln\rho\right]\frac{d\gamma_e}{dr} \,, \tag{23}$$

Next the temperature changes during an adiabatic process in an ionizing gas will be derived. Consider, as a definition of μ,

$$P = \frac{k}{m_H}\frac{\rho T}{\mu} \,. \tag{24}$$

Differentiating, one has

$$\frac{dP}{P} = \frac{dT}{T} + \frac{d\rho}{\rho} - \frac{d\mu}{\mu} \,. \tag{25}$$

Eliminating dP/P from Eqs. (20) and (25) one now has

$$\frac{dT}{T} = (\gamma_e - 1)\frac{d\rho}{\rho} + \frac{d(\gamma_e - 1)}{\gamma_e - 1} + \frac{d\mu}{\mu} \,. \tag{26}$$

As above, if one considers the coefficient of $d\rho/\rho$ constant, an approximate solution to Eq. (26) is

$$T \approx K(\gamma_e - 1)\,\mu\rho^{\gamma_o - 1} \,, \tag{27}$$

where $\gamma_e(\rho, T)$ is near $\gamma_e(\rho_o, T_o) = \gamma_o$ and K is a constant. For γ_e and μ constant one obtains the standard solution to Eq. (26) with $\gamma_e(\rho_o, T_o)$.

Consequently, the convective temperature gradient with $\gamma_e(\rho_o, T_o)$ in Eq. (5) is correct only for small changes in T and ρ about T_o and ρ_o. Here γ_e is used because it reflects the properties of a real gas where the correct adiabatic IEEOS temperature gradient is obtained by substituting Eq. (20) into Eq. (26) for $d\rho/\rho$, or

$$\frac{dT}{dr} = \frac{\gamma_e - 1}{\gamma_e} \frac{T}{P} \frac{dP}{dr} + \frac{T}{\gamma_e} \frac{d\gamma_e}{dr} + \frac{T}{\mu} \frac{d\mu}{dr} . \tag{28}$$

In the analysis of shock waves moving through the outer layers of a star, one is concerned with the velocity of sound C in stellar material. From Eq. (20),

$$dP = \gamma_e \frac{P}{\rho} d\rho + \frac{P}{\gamma_e - 1} d\gamma_e . \tag{29}$$

Note, first, from Eq. (29) that the pressure gradient during an adiabatic process in an ionizing gas can be altered when there is a change in γ_e. Multiplying the last term in Eq. (29) by $d\rho/d\rho$, one has

$$dP = \gamma_e \frac{P}{\rho} d\rho + \frac{P}{\gamma_e - 1} \frac{d\gamma_e}{d\rho} d\rho ,$$

or (30)

$$dP = \left(\gamma_e \frac{P}{\rho} + \frac{P}{\gamma_e - 1} \frac{d\gamma_e}{d\rho}\right) d\rho .$$

Now $C^2 = dP/d\rho$ along an adiabat, or

$$C^2 = \gamma_e \frac{P}{\rho} + \frac{P}{\gamma_e - 1} \left(\frac{d\gamma_e}{d\rho}\right)_{adiabat} \tag{31}$$

Note that for $\gamma_e = \gamma_e(\rho, T)$,

$$\left(\frac{d\gamma_e}{d\rho}\right)_{adiabat} = \left(\frac{\partial\gamma_e}{\partial\rho}\right)_T + \left(\frac{\partial\gamma_e}{\partial T}\right)_\rho \left(\frac{dT}{d\rho}\right)_{adiabat}$$

Hence, Eq. (31) can also be written as

$$C^2 = \gamma_e \frac{k}{m_H} \frac{T}{\mu} + \frac{P}{(\gamma_e - 1)} \left(\frac{d\gamma_e}{d\rho}\right)_{adiabat} \tag{32}$$

The variations of ρ, γ_e, T, μ, and P along a stellar profile are given in Figs. 1 through 5. Clearly, Eq. (32) equals the standard expression for the speed of sound only in the $T - \rho$ regions where γ_e is constant.

Finally, the quantity Unsöld called the effective value of the ratio of specific heats Γ is not the γ_e of this report (17). Unsöld defines Γ by

$$\frac{\Gamma - 1}{\Gamma} = \left[\frac{d(\ln T)}{d(\ln P)}\right]_{adiabat} \tag{33}$$

From Eqs. (20) and (26),

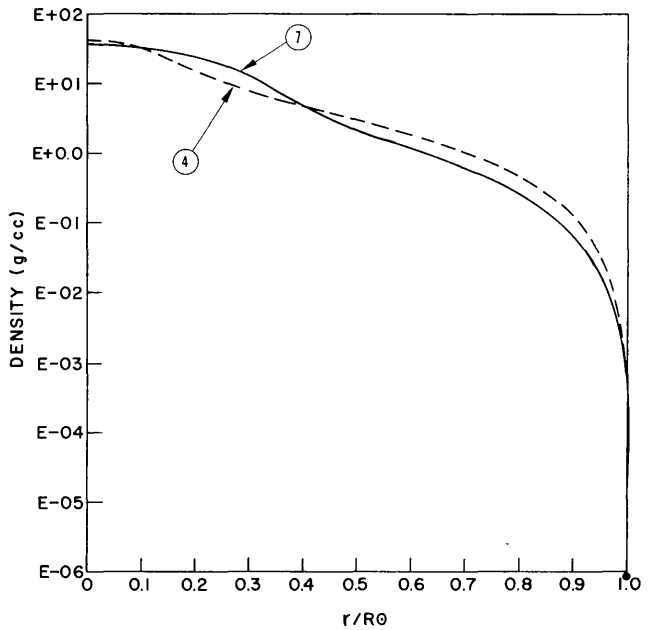

Fig. 1 - Density ρ versus relative radius $r/R_\odot$. The numbers on the curves refer to the corresponding cases of Tables 1 and 2.

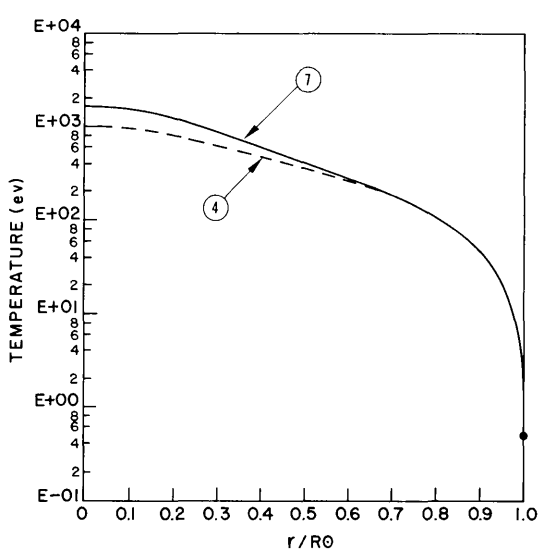

Fig. 2 - Temperature T versus relative radius $r/R_\odot$. The numbers on the curves refer to the corresponding cases of Tables 1 and 2.

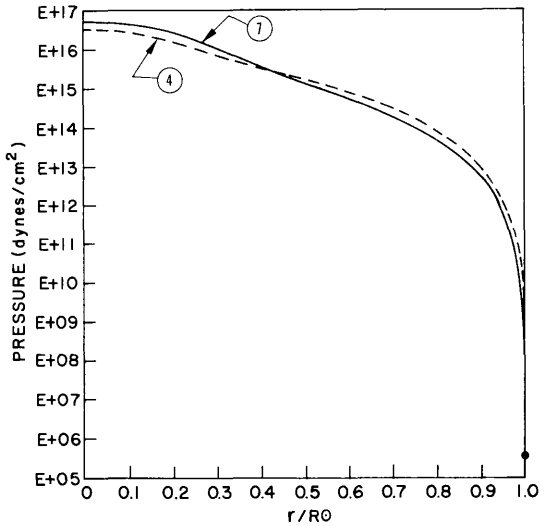

Fig. 3 - Pressure P versus relative radius $r/R_\odot$. The numbers on the curves refer to the corresponding cases of Tables 1 and 2.

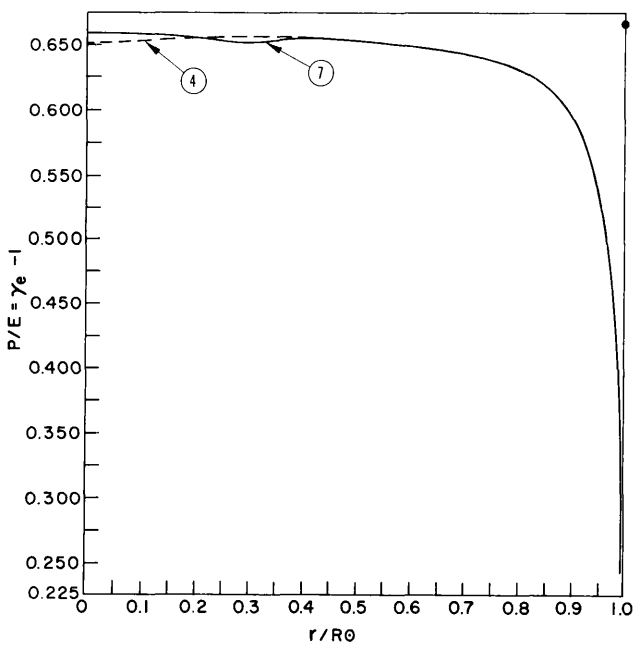

Fig. 4 - $\gamma_e - 1$ versus relative radius $r/R_\odot$. The numbers on the curves refer to the corresponding cases of Tables 1 and 2.

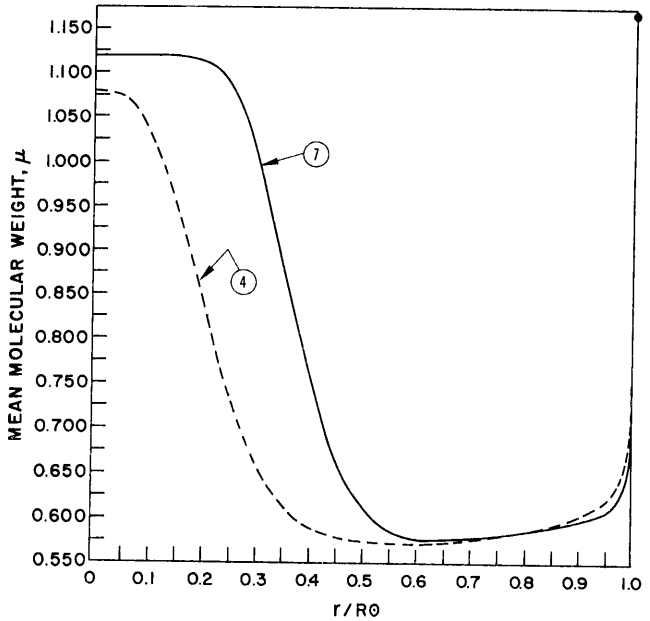

Fig. 5 - Mean molecular weight μ versus relative radius $r/R_\odot$. The numbers on the curves refer to the corresponding cases of Tables 1 and 2.

$$\frac{dT}{T} = \frac{\gamma_e - 1}{\gamma_e}\frac{dP}{P} + \frac{d\gamma_e}{\gamma_e(\gamma_e - 1)} + \frac{d\mu}{\mu} . \tag{34}$$

Hence, γ_e and Γ are equal only when γ_e and μ are constant.

For a review of the theoretical problems of the equation of state for matter at high densities and temperatures, see Brush (18) in Vol. 1 of the present series.

Opacity

With the more detailed output of the IEEOS available, the opacity can be calculated using the ionic distribution resulting from the determination of the IEEOS. Assuming a single excited electron for each ion, the Kramer opacity formula for bound-free transitions can be expanded and written as (with $i = 1$ for neutral atoms, 2 for singly ionized atoms, etc.)

$$K_1 = K_o N_e \left(\sum_{j=1} \sum_{i=1}^{Z_j} N_{ij}\, i^2 \right) \Big/ \rho T^{3.5} \tag{35}$$

with total K given by

$$K = K_1 + (6.307 \times 10^{-25} N_e/\rho) , \tag{36}$$

where K_o will be an input parameter. The power of N_e in K_1 was varied, but the results were not significantly different; and with the uncertainties in the opacity formulation itself and the relative abundances of the elements, it was not felt worthwhile to pursue this

aspect for the present investigation. The concept of a mean Gaunt factor would justify using the parameter K_o. Results where opacity fits based on relative mass abundances were used were not significantly different from those obtained using Kramer's formula. Furthermore, bound-free opacities for hydrogen at densities greater than 10 g/cc would have to be explained away. (For hydrogen at $\rho = 2.7$ g/cc the radius of the mean atomic volume equals the radius of the first Bohr orbit.)

For the photosphere, fits were made to the Chandrasekhar and Münch (19) absorption coefficients for neutral and negative hydrogen ions. With these fits the opacity was calculated using their expression, recalling that the abundance of neutral hydrogen and the electron pressure are calculated in the IEEOS. For discussions of opacity calculations, see Cox (20) and Armstrong, et al. (21).

Energy Generation

The expressions for energy production used are those given by Schwarzschild (6b). With T given in eV these equations become

$$\epsilon_{pp} = 4.88^7 X^2 \rho T^{-2/3} \exp(-149.0/T^{1/3}) \tag{37}$$

and

$$\epsilon_{cn} = 1.85^{30} X X_{CN} \rho T^{-2/3} \exp(-671.0/T^{1/3}) , \tag{38}$$

with the total of the two cycles given by

$$\epsilon = \epsilon_{pp} + \epsilon_{cn} .$$

In the present study the numerical multiplying constants in Eqs. (37) and (38) were introduced as input parameters ϵ^o_{pp} and ϵ^o_{cn}, with ϵ^o_{cn} also including X_{CN}. In this study X_{CN} was not allowed to vary as the relative mass abundance of hydrogen alone varied because the ratio

$$(H + 4He)/(C + N) \tag{39}$$

should remain constant — and not $H/(C+N)$ — if the initial abundance of helium was zero. For finite initial abundance of He,

$$\frac{(H^o + He^o)_{initial} - H_{burned} + 4He_{produced}}{C+N} \approx \text{constant}. \tag{40}$$

If one neglects the He in the sun's photosphere and determines $H/(C+N)$, then for the present sun the $C+N$ abundance in the interior is not correct unless one uses Eq. (39). The same arguments hold for all elements whose abundances are not changing due to nuclear reactions. For the present calculations X_{CN} was assumed to be 0.005 and considered part of the ϵ^o_{cn} parameter. For a review of the sources of stellar energy, see Reeves (22).

RESULTS

At first, attempts were made to calculate the mass and radius of the sun using a homogeneous mixture of elements. This proved impossible; so the helium abundance was inserted as the above parameter. Then with an assumed $T_c = 1000$ eV, ρ_c and He were varied in the first attempts to calculate $M_\odot$ and $R_\odot$. Some results for this T_c are shown in Table 1. For computational speed, δ was set at 0.1; the relative error in the

Table 1
Results with T_c = 1000 eV, He = 5^{10} [1 + 29 exp (-10.0 $M_r/M_\odot$)]

Case	ρ_c	T_f	P_e	M	L	R	ρ_f	δ
1	42.9	0.489	26.7	1.991^{33}	0.070^{33}	6.939^{10}	2.50^{-6}	0.1
2	42.9	0.511	15.1	1.992^{33}	0.070^{33}	6.942^{10}	2.20^{-7}	0.1
3	41.8	0.488	25.6	1.994^{33}	4.02^{33}	6.966^{10}	2.47^{-6}	0.1
4	41.825	0.496	39.9	1.990^{33}	4.011^{33}	6.955^{10}	3.67^{-6}	0.05

IEEOS iterations was set at 0.001, and the relative error in the calculation of P_{j+1} in the IEEOS for the determination of ρ_{j+1} was also set at 0.001. With these computational parameters, profiles were calculated in about 5 min with the IBM 7094 -- including 15 plots of various quantities versus ρ, T, and $r/R_\odot$. Variations from the above computational parameters will be discussed below.

In case 2 of Table 1 the Chandrasekhar-Münch photospheric opacity was arbitrarily reduced by a factor of 20 in order to force the radiative temperature gradient to be used. Otherwise, in all the present results the convective gradient controlled the temperature calculations throughout the outer 70 to 80% of the sun's radius. In case 3, ϵ^o_{pp} was increased by a factor of 60 (with an appropriate reduction in K_o) in order for the calculated energy generation to match the luminosity.

Table 2 presents the initial results for T_c = 1650 eV (=19.1×10^6 °K). (A slight increase in T_c would result in the correct luminosity, but it was not felt significant in the initial phase of this study to search for this T_c.) In Table 3 are presented results with variations on input quantities and with increased accuracy in the IEEOS calculations -- with resulting 50 to 100% increase in computational time. Note that there is only about 1.5% change in both the mass and radius from the results in Table 2. In cases where both the IEEOS and the ρ_{j+1} determination were run with relative errors of 10^{-4}, there were essentially no changes in the mass and radius as compared with the Table 2 results, but the computational time was 3 to 5 times greater, depending on the value of δ. Also in Table 3, cases 8 through 11 indicate the contribution of electrons from hydrogen to the photospheric electron pressure. Note that the increase in electron pressure is about 14 dynes/cm^2 -- the electron pressure given in various photospheric models at T ≈ 5800°K. Also note that the electron pressure in Minnaert's adopted photospheric model (5) is that of cases 1, 3, 8, 9, 12, 14, and 18.

Table 4 demonstrates the effect of decreasing δ. Note that the results are unchanged except for the final electron pressure and mass density. Studies at NRL demonstrated

Table 2
Results with T_c = 1650 eV, δ = 0.1, He = 5.0^{10} $\{1 + 37.0 \exp[-D_2 (M_r/M_\odot)^3]\}$

Case	ρ_c	D_2	T_f	ρ_f	P_e	M	L	R
5	30.0	4.0	0.4871	4.957^{-7}	10.43	1.990^{33}	2.372^{33}	6.616^{10}
6	35.2	8.0	0.4889	8.363^{-7}	15.10	1.989^{33}	2.566^{33}	6.970^{10}
7	36.8	9.15	0.4895	9.169^{-7}	16.12	1.988^{33}	2.625^{33}	6.962^{10}

Table 3
Results with T_c = 1650 eV, He = 5.0^{10} $\{1 + 37.0 \exp[-D_2(M_r/M_\odot)^3]\}$, δ = 0.1. IEEOS Relative Error = 10^{-4}, P = Planck Partition Function, U-F = Urey-Fermi Partition Function, and Metals = Relative Number Abundance of Metals.

Case	ρ_c	T_f	ρ_f	P_e	M	L	R	D_2	Part	Metals
8	35.2	0.4888	9.271^{-7}	29.93	2.021^{33}	2.567^{33}	6.855^{10}	8.0	P	8.7^{7}
9	35.2	0.4959	9.466^{-7}	28.75	2.022^{33}	2.568^{33}	6.860^{10}	8.0	P	5.26^{7}
10	35.2	0.4958	9.108^{-7}	15.79	2.023^{33}	2.569^{33}	6.867^{10}	8.0	P	1.0^{7}
11	35.2	0.4872	9.610^{-7}	15.39	2.024^{33}	2.569^{33}	6.868^{10}	8.0	P	—
12	35.2	0.4978	1.493^{-6}	26.68	2.026^{33}	2.569^{33}	6.905^{10}	8.0	U-F	—
13	30.0	0.4899	8.607^{-7}	15.19	2.017^{33}	2.374^{33}	6.631^{10}	4.0	U-F	—

Table 4
Results with T_c = 1650 eV, He = 5.0^{10} $\{1 + 37.0 \exp[-D_2(M_r/M_\odot)^3]\}$, Planck Partition Function

Case	δ	T_f	ρ_f	P_e	M	L	R	IEEOS Error
ρ_c = 35.2, D_2 = 8.0								
6	0.1	0.4889	8.363^{-7}	15.10	1.989^{33}	2.566^{33}	6.970^{10}	10^{-3}
14	0.05	0.4953	1.346^{-6}	23.43	1.989^{33}	2.566^{33}	6.967^{10}	10^{-3}
15	0.02	0.4993	2.936^{-6}	39.19	1.989^{33}	2.566^{33}	6.962^{10}	10^{-3}
With Metals (as in Case 9)								
9	0.1	0.4959	9.466^{-7}	28.75	2.022	2.568	6.860	10^{-4}
16	0.05	0.4951	1.510^{-6}	37.86	2.022	2.568	6.857	10^{-4}
ρ_c = 30.0, D_2 = 4.0								
17	0.1	0.4955	5.606^{7}	19.48	2.004	2.372	6.538	10^{-4}
18	0.05	0.4967	9.608^{-7}	27.89	2.004	2.372	6.535	10^{-4}

that δ = 0.1 yields about the optimum balance between truncation and roundoff errors. It was shown that in the photosphere, $\Delta P/P$ controls Δr with $\Delta T/T \approx 0.1\ (\Delta P/P)$. Hence, $\delta > 0.1$ makes ΔP nonlinear (the exact quadratic term is needed); and $\delta < 0.1$ leads to a loss of significance in the ΔT calculation.

Table 5 compares calculations from case 12 of Table 3 in the photosphere interior to the T = 0.495 eV radius and the outer envelope with results from Allen (23). It should be emphasized that the present results were an incidental consequence of a numerical search for mass and radius agreement that began at the center of the sun and calculated

Table 5
Photosphere Interior to the T = 0.495 eV Radius and the Outer Envelope Calculated in Case 12 of Table 3 Compared with Results from Allen

From Case 12, Table 3					Taken from Allen		
$r/R_\odot$	$(R-r)/R_\odot$	(R - r) (km)	T (Convective Gradient) (°K)	$\gamma_e - 1$	h (km)	T (°K)	h + 260 (km)
0.99227	—	—	5,770	0.6661	-260	5,800	—
0.99216	0.0001	70	6,990	0.6621	-330	7,000	-70
0.99121	0.0011	770	15,000	0.3325	-1000	14,000	-740
0.98927	0.0030	2090	23,500	0.2560	-2000	20,000	-1740
0.98140	0.0109	7600	52,000	0.3354	-7000	43,000	-6740

out to the photosphere. Furthermore, there were at least six calculations between 5770 and 6990°K (not printed out). Quite generally, the region where $\gamma_e - 1$ was below 0.333 was between 0.0011 $R_\odot$ and 0.011 $R_\odot$ below the surface T = 0.5 eV, and the minimum γ_e printed out occurred between 0.002 $R_\odot$ and 0.004 $R_\odot$.

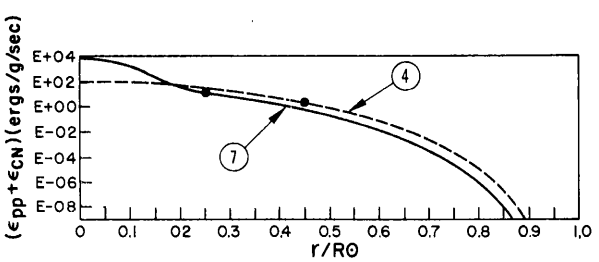

Fig. 6 - Energy generation rate ϵ versus relative radius $r/R_\odot$. The numbers on the curves refer to the corresponding cases of Tables 1 and 2. The dots indicate the radius at which $L_r \approx L_\odot$.

The calculated internal structure is plotted in Figs. 1 through 8. The numbers on the graphs refer to the corresponding cases of Tables 1 and 2. The graphs, with their subtitles, are self-explanatory. Commenting only on Fig. 7 here, we note that the three curves represent the three types of solutions obtained. Where the ratio indicated is less than 1, the radiative temperature gradient is used. Case 4 shows the radiative temperature gradient is used for the first 20% of the radius; in case 5 the radiative gradient is used between 20 and 30% of the radius, and in case 7 the convective gradient is used throughout. Matching the mass and radius is easiest with solutions like case 7. Solutions like cases 4 and 5 required adjusting K_o to four significant figures. Under no circumstance could complete radiative solutions be obtained.

DISCUSSION

Allen (23) gives the current values of $M_\odot$, $R_\odot$, and $L_\odot$ as

$$M_\odot = (1.989 \pm 0.002)^{33} \text{ g},$$

$$R_\odot = (6.9598 \pm 0.0007)^{10} \text{ cm},$$

and

$$L_\odot = (3.90 \pm 0.04)^{33} \text{ ergs/sec}.$$

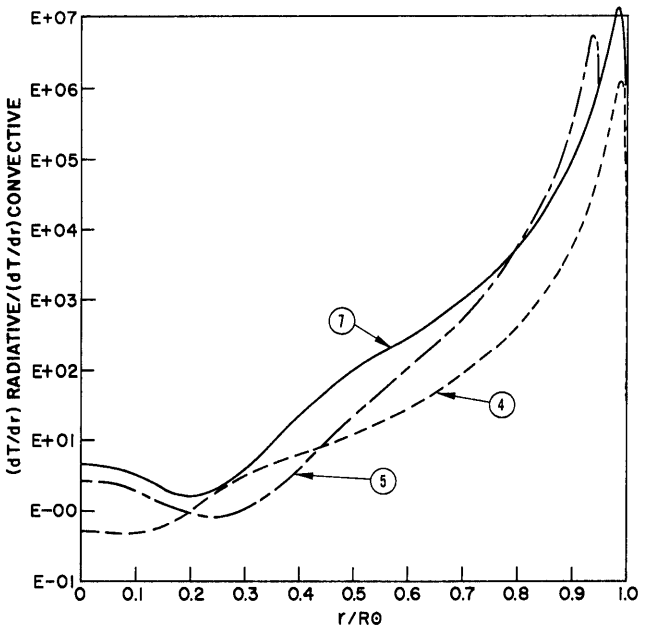

Fig. 7 - Ratio of the radiative-to-convective temperature gradients versus relative radius $r/R_\odot$. The numbers on the curves refer to the corresponding cases of Tables 1 and 2.

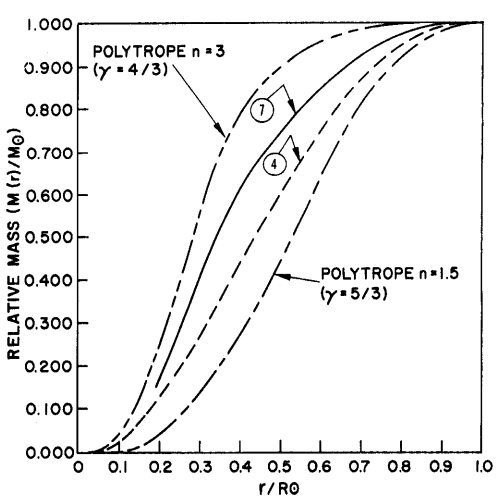

Fig. 8 - Relative mass versus relative radius $r/R_\odot$. The numbers on the curves refer to the corresponding cases of Tables 1 and 2.

Also from Allen (23) and Schwarzschild (6) central densities of the sun are given values of about 98 to 158 g/cc and central temperatures about 13×10^6 to 20×10^6 °K. The present investigations began with published central T's and ρ's. Calculating $M_\odot$ was relatively easy. Calculating $M_\odot$ and $R_\odot$ was impossible until assumed central densities were lowered and He profiles inserted as a parameter to vary μ as discussed in the last section. Since the calculation of $M_\odot$, $R_\odot$, and $L_\odot$ is not unique because of various uncertainties, it is in order to comment about a solar solution and the solar solution. Any solution in which $M_\odot$, $R_\odot$, and $L_\odot$ are satisfied will be referred to as a solution. This will include solutions with massless envelopes. Clearly the solution is one that reproduces not only the

aforementioned quantities but also the photosphere; and, further, the solution should be compatible with other observed properties of the sun. The ability to do this would of course establish a formalism for calculating profiles of more distant stars where less detailed observations can be made. This in turn will lead to a better understanding of sizes, masses, and the presence or absence of pulsations and explosions in stars.

As for $L_\odot$, this quantity is automatically satisfied in a solution in which one calculates the effective solar temperature T_e at a radius $R_\odot$. However, in the solution, one should also be able to calculate the luminosity from the energy generation cycles. In fact, if one knew $\rho(r)$ exactly, Eqs. (1) and (2) would yield the solution. Then, from the equation of state, one would obtain $T(r)$ and then obtain $L(r)$ from the energy generation cycles. But since $\rho(r)$ is not known either, Eq. (4) or (5), or possibly another relationship, is needed to establish a complete solution. This is not new, but the author wishes to emphasize that calculation of $L_\odot$ by means of Eq. (3) will not yield the solution unless one knows $\rho(r)$ as well as $\epsilon(r)$ correctly.

Let us assume we know $\epsilon(\rho, T, X, X_{CN})$ accurately enough. The first problem is then to establish the $\rho(r)$, $T(r)$, $X(r)$, and $X_{CN}(r)$ that yield $M_\odot$, $L_\odot$, and $R_\odot$. If this solution is not unique, then one must look to other observable quantities such as the structure of the photosphere with the H/He and H/metals ratios and electron pressure as possible calculable quantities. It is felt that the ability to do this will indicate a narrow range of solutions to the solar problem, approximating the solution.

The sun as a possible test for the IEEOS in a $T-\rho$ range beyond the reach of terrestrial laboratories has not only been shown to be possible but also indicated (through present results) areas in which better observations could lead to the solution. The results in Tables 1 through 6 indicate that the determination of H/He, H/metals, and electron pressure down to two optical depths in the photosphere would yield quantities calculable from the center.

With the uncertainty of the H/He ratio in the photosphere, one should consider solutions with the two extreme values of 20 and 5. The solutions in Tables 1 through 5 result in H/He ratios of 20 in the photosphere, except the cases with $\rho_c = 30$ g/cc. In order to obtain solutions with H/He ≈ 5 in the photosphere and $T_c = 1650$ eV, one must go to lower values of ρ_c leading to still lower calculated luminosities.

Table 6
Results with Minnaert's Helium (H/He = 5.55) and Metal (1.12^7) Abundance in the Photosphere; $He = 18.0^{10}\{1 + 37 \exp[-D_2(M_r/M_\odot)^3]\}$, Planck Partition Function $\delta = 0.1$, and IEEOS Relative Error = 10^{-3}

Case	D_2	D_3	T_c (eV)	ρ_c	T_f	ρ_f	P_e	M	L	R
19	7.0	3	1750.0	24.5	0.4873*	1.861^{-7}	5.905	1.962^{33}	1.668^{33}	7.009^{10}
20	7.5	4	1800.0	24.5	0.4905	1.739^{-7}	6.306	1.989^{33}	2.899^{33}	6.926^{10}
21	10.0	3	1810.0	29.5	0.4994	2.637^{-7}	10.27	1.989^{33}	3.532^{33}	7.004^{10}
22	10.0	3	1820.0	30.0	0.4873	2.559^{-7}	7.052	1.989^{33}	3.964^{33}	6.967^{10}
23	10.0	3	1819.0	30.0	0.4932	2.619^{-7}	8.519	1.9865^{33}	3.921^{33}	6.960^{10}
24	10.0	3	1818.5	30.0	0.4919	2.615^{-7}	8.193	1.985^{33}	3.900^{33}	6.957^{10}
25	10.0	3	1818.0	30.0	0.4992	2.663^{-7}	10.29	1.984^{33}	3.880^{33}	6.954^{10}

*Radiative at last point printed out ($\nabla_R T/\nabla_C T = 0.997$).

Two aspects of the IEEOS have been shown to significantly affect the solutions. Cases 11 and 12 of Table 3 illustrate the effect the approximate partition functions have on the calculated P_e in the photosphere. A third variation was to use constant ground state degeneracies only as the partition functions, which lead to an electron pressure about 15% higher than that of case 12 at the same temperature. However, the truncation and roundoff errors might also have influenced the results.

The second and most interesting changes were those due to the effect of the high-density formulation of the IEEOS. Case 1 recalculated without the high-density formulation resulted in a 10% increase in both the mass and radius. Cases 5 and 6 recalculated without the high-density formulation lead to 5% decreases in both mass and radius. Had central densities of 100 g/cc or higher led to more complete solutions, the effect would have been much greater. Furthermore, at 100 g/cc there results about 10% neutral hydrogen atoms with the standard Saha equation; hence one would have to assume that all the hydrogen and helium atoms were stripped. The presently used modified Saha equation not only appears to lead to the correct equation of state throughout the $T-\rho$ range of stellar profiles but also yields the more detailed information needed in calculations of opacity and energy generation.

With regard to the photosphere results in Table 5, the present code prints out results when r is equal to or greater than a multiple of the initial Δr. The entries in Table 5 from case 12 are, reading in the negative r direction, the last point and then the 2nd, 3rd, 5th, and 13th points from the last actually printed out. Specifically, between points 3 and 2 and between 2 and 1, the pressure gradient controlled the Δr with at least 23 points and 6 intermediate points calculated, respectively, but not printed out. The agreement of the temperature gradients between one-half and two optical lengths (τ) is even more remarkable, because the present calculation used the real-gas convective gradient (with γ_e).

In addition, consider the depth at which $\gamma \approx 4/3$. The origin of solar granulation is believed to be about 300 km below the visible photosphere (24), hence, about 300 km below one optical length. From Allen (23) this would be at about $h = -600$ km. Note in Table 5 how close this approximate figure is to the depth in the present calculations where $\gamma_e \approx 4/3$. This suggests that the perturbations giving rise to the upward movement of gases could indeed have their origins in the region where $\gamma_e \approx 4/3$ — the region given by Woolley and Stibbs (17) as the convective zone where the mean opacity is independent of the optical depth.

With the success in calculating photosphere temperature gradients with γ_e discussed above, it was decided to try for solutions with Minnaert's photospheric H/He ratio of 5.55 and metals abundance of 1.12^7. The results are given in Table 6. With a decrease in δ and in the relative error, the mass and radii changed as discussed above (see Table 4).

Stability Conditions Derived From Real-Gas Properties

On the other hand, stability to convective motion can be expressed in terms of perturbations at constant γ_e and/or constant μ. Consider two equations for P along the equilibrium profile:

$$P \approx B\rho^{\gamma_e} \tag{41}$$

and

$$P = \frac{k}{m_H}\frac{\rho T}{\mu}, \tag{42}$$

where B is a constant and m_H is the mass of a hydrogen atom. Differentiating, one has

$$\frac{d\rho}{dr} \approx \frac{\rho}{\gamma_e P}\frac{dP}{dr} - \frac{\rho}{\gamma_e}(\ln \rho)\frac{d\gamma_e}{dr} \tag{43}$$

and

$$\frac{d\rho}{dr} = \frac{\rho}{P}\frac{dP}{dr} - \frac{\rho}{T}\frac{dT}{dr} + \frac{\rho}{\mu}\frac{d\mu}{dr} . \tag{44}$$

In an isothermal perturbation or a perturbation in which the temperature change is near to that given by the convective gradient, Eq. (44) can be written as

$$\frac{d\rho}{dr} = f(\rho, T)\frac{dP}{dr} + \frac{\rho}{\mu}\frac{d\mu}{dr} \tag{45}$$

with $f(\rho, T) > 0$.

Now a perturbation in a positive Δr direction in which the perturbed density is less than the equilibrium density at $r + \Delta r$ is unstable, and one where the perturbed density is greater than the equilibrium density at $r + \Delta r$ is stable. From Eq. (43), in a region where $\rho < 1$ and $d\gamma_e/dr > 0$ along the equilibrium profile, a perturbation at, for example, constant γ_e is unstable. Also, in a region where $\rho > 1$ and $d\gamma_e/dr < 0$, a perturbation at constant γ_e is unstable. From Eq. (44), in a region where $d\mu/dr > 0$, a perturbation at constant μ is unstable, whereas in a region with $d\mu/dr < 0$ a perturbation at constant μ is stable. In all of the present results the region where both $d\gamma_e/dr$ and $d\mu/dr$ are very large and positive is just below the photosphere, with $d\mu/dr \approx 0$ at $T \approx 0.5$ eV. Consequently, in the region between minimum γ_e and $r \approx R_\odot$, either a constant γ_e or constant μ perturbation to $r + \Delta r$ would lead to a decrease in density greater than the decrease along the equilibrium profile; hence such a displaced element of matter would be less dense than that of the surrounding matter and would continue to rise. In fact, a perturbation with any change in γ_e or μ less than the change along the equilibrium profile — including decreases in γ_e or μ — would satisfy the stability criteria just given for constant γ_e or μ perturbations in this region of positive $d\gamma_e/dr$ and $d\mu/dr$.

In general, from Eqs. (43) and (45) stability criteria can be established in terms of changes in γ_e and μ being either less than, equal to, or greater than the corresponding changes along the equilibrium profile.

The region below minimum γ_e and above the inner point where $\gamma_e \approx 4/3$ has $d\gamma_e/dr < 0$ and $d\mu/dr > 0$ and hence might be a region of quasi stability. Consequently, it appears that the perturbations leading to the observed granulation have their origins in the outer (approximately 0.2%) portion of the sun's radius and not throughout the entire zone where $\gamma_e \leqq 4/3$ as discussed above. In the present results the temperatures at minimum γ_e range from about 1.6 to 2 eV. Since no helium lines are observed in normal granulation, either the granular matter does not come from this depth or, if so, it stays very close to the equilibrium profile temperature.

The above analysis further suggests that perturbations leading to solar flares and other solar prominences have deeper origins — possibly in the region between minimum γ_e and the depth where $d\mu/dr \approx 0$. In this region the present results have $\rho < 1$, $d\gamma_e/dr < 0$, and $d\mu/dr > 0$. The interplay between the stabilizing and unstabilizing effects of $d\gamma_e/dr$ and $d\mu/dr$, respectively, could account for the relative rarity (with respect to granulation) of the various solar eruptions. The observation of He lines in the spectra of prominences is not incompatible with matter coming from this region, for in the present results the temperature at minimum γ_e is about 2 eV and the temperature near $d\mu/dr \approx 0$ is about 100 to 300 eV. Furthermore, the temperatures at the inner point where $\gamma_e \approx 4/3$ range from 4 to 5 eV. Consequently, near-isothermal eruptions, even from the lower part of the region where $\gamma_e < 4/3$, could account for the helium spectra in prominences.

Finally, from Fig. 5, throughout the core $d\mu/dr \lesssim 0$ and $d\gamma_e/dr \lesssim 0$ with $\rho > 1$; hence the profile would be stable to constant μ and γ_e perturbations.

Mass -- Central Density Relationship

To avoid a lot of trial-and-error calculations an approximate relationship was sought in which the mass could be predicted from the T_c and ρ_c. The constant portion of the case 4 curve in Fig. 7 suggests that the ratios of temperature gradients might be useful. Writing the radiative gradient as $\nabla_R T$ and the convective gradient as $\nabla_C T$, we have from Eqs. (4), (5), and (1) that

$$\nabla_R T \propto \frac{K\rho L_r}{T^3 r^2} \tag{46}$$

and

$$\nabla_C T \propto \frac{\gamma - 1}{\gamma} \frac{T}{P} \frac{\rho M_r}{r^2} . \tag{47}$$

For r small and $\epsilon \sim \epsilon^o_{pp} X_H^2 \rho_c T_c^4$, $L_r \sim \rho_c \epsilon r^3$, $N_e \sim \rho_c$, and $K \sim K_o \rho_c / T_c^{3.5}$. Also, $P_c \sim \rho_c T_c$, $M_r \sim \rho_c r^3$, and Eqs. (46) and (47) indicate that

$$\nabla_R T \propto \frac{\epsilon^o_{pp} K_o \rho_c^4 X_H^2}{T_c^{2.5}} \tag{48}$$

and

$$\nabla_C T \propto \frac{\gamma - 1}{\gamma} \rho_c r . \tag{49}$$

Hence,

$$\frac{\nabla_R T}{\nabla_C T} \propto \epsilon^o_{pp} K_o X_H^2 \frac{\gamma}{\gamma - 1} \frac{\rho_c^3}{T_c^{2.5}} \tag{50}$$

with the r-dependence dropping out. Earlier calculations indicated that as ρ_c increased, M decreased, hence the working relationship should be given by

$$M \frac{\nabla_R T}{\nabla_C T} \approx \text{constant} , \tag{51}$$

or

$$M \epsilon^o_{pp} K_o X_H^2 \frac{\gamma}{\gamma - 1} \frac{\rho_c^3}{T_c^{2.5}} \approx \text{constant} . \tag{52}$$

Starting with solution case 1, Eq. (52) predicted that $M = M_\odot$ with $T_c = 1170$ eV and $\rho_c = 49.0$ g/cc. The numerical calculations actually yielded $M = 1.989^{33}$ g and $R = 6.235^{10}$ cm. At $T_c = 1300$ eV, $\rho_c = 53.5$ g/cc; the numerical calculations gave $M = 2.078^{33}$ g and $R = 5.995^{10}$ cm. Finally, at $T_c = 1400$ eV, $\rho_c = 56.8$ g/cc; the numerical calculations resulted in $M = 2.336^{33}$ g and $R = 6.060^{10}$ cm. Note that the large deviations occur as the temperature increases to the range where ϵ does not vary as T^4. In general, instead of Eq. (52), it was found most convenient to use (with an assumed T_c)

$$M\rho_c^n \approx \text{constant}, \tag{53}$$

with n to be determined. With two trial calculations, n is obtained from

$$M_1 \rho_1^n = M_2 \rho_2^n . \tag{54}$$

With this value of n, the central density that leads to a value of M close to $M_\odot$ is given by

$$\rho_c \approx \rho_2 \left(\frac{M_2}{M_\odot}\right)^{1/n} . \tag{55}$$

In general the numerical determination of R obtained starting with the ρ_c from Eq. (55) was not equal to $R_\odot$. Then it was necessary to vary the helium profile, and usually ρ_c again, before $M_\odot$ and $R_\odot$ could be calculated simultaneously.

Results With Improved Programs

During December 1964 an improved version of the solar code was put into operation on the more accurate and faster CDC 3600 and CDC 6600 electronic computers. The larger numbers available permitted relaxation of overflow-underflow tests necessary in the IBM 7094 version of the solar code.

The physical improvement added pertains to the high-density formulation of the EOS (13). In the term $\Phi(\rho) = \Phi(r_o) = \exp[-f(a_n, r_o)]$, the $f(a_n, r_o)$ was chosen to be proportional to the "size" of the neutral atom. Now, the $f(a_n, r_o)$ is entered as proportional to the radius of maximum radial charge density as determined by self-consistent field calculations for each shell (25). Since the radius of the mean atomic volume r_o is used, the author felt that the mean position of the electron in the isolated atom orbital is the point that would reflect the density effect in the high-density formulation. Hence, for s-states, 1.5 times the radius of maximum charge density was used as a first order approximation in $f(a_n, r_o)$.

With greater speed and accuracy, the new calculations were carried out with a relative error in the IEEOS of 10^{-4}. Furthermore, a more recent H/He ratio and metals abundance were used, namely, Aller's (26) H/He photospheric abundance ratio of 7 and metals abundance of 7.37^7. Some results are shown in Table 7. Note that there are only slight differences from the results of case 24 of Table 6.

Table 7
Results with the Improved CDC 3600 Code and with Aller's Helium (H/He = 7) and Metal (7.37^7) Abundances in the Photosphere; He = 14^{10} $\{1 + 42 \exp[-10(M/M_\odot)^{3.5}]\}$, and IEEOS Relative Error = 10^{-4}

Case	T_c (eV)	ρ_c	T_f	ρ_f	P_e	M	L	R
26*	1809	29.9	0.4667	1.410^{-7}	4.053	1.9896^{33}	3.90^{33}	6.931^{10}
27†	1809	29.9	0.4956	3.044^{-7}	12.93	1.9796^{33}	3.90^{33}	6.890^{10}
28‡	1809	29.9	0.4431	2.504^{-7}	3.563	1.9896^{33}	3.90^{33}	6.926^{10}

* δ = 0.2; U-F partition function, six elements including Si and Fe.
† δ = 0.1; Planck partition function, five elements including Si.
‡ δ = 0.1; U-F partition function, five elements.

Next, the photospheric calculations from case 28 (Table 7) of T and P_e are given in Table 8 and in Fig. 9, where they are compared with several empirical solar models from Fig. 5-4 of Aller (26).

Table 8
Values of Temperature and Electron Pressure in the Photosphere Calculated in Case 28, Table 7

R/R⊙	T (eV)	P_e
0.99512527	0.4431	3.563
0.99506277	0.4887	11.63
0.99500027	0.5581	70.02
0.99496902	0.5926	159.9
0.99487526	0.6946	1.249^{3}
0.99478152	0.7915	5.725^{3}
0.99468777	0.87935	1.76^{4}

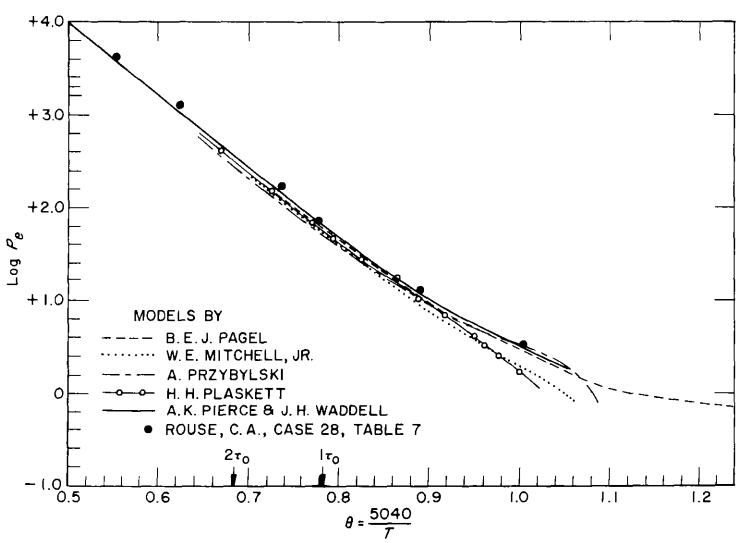

Fig. 9 - Relation between θ = 5040/T and electron pressure for several empirical solar model atmospheres. Included are present results from case 28, Table 7. (Other curves are from Fig. 5-4 of Ref. 24.) The τ_o refer to optical lengths.

Calculations completed in January 1965 (27) with abundances of elements calculated relative to H + 4He yielded the following: T_c = 1815 eV, ρ_c = 29.85 g/cc, M = 1.989^{33} g ≡ M⊙, L = 3.902^{33} ergs/sec (w/ϵ^{o}_{cn} = 8.86^{27}), R = 6.953^{10} cm = 0.9991R⊙, T_f = 0.442 eV = 5,130°K, ρ_f = 2.788^{-7} g/cc, and P_e = 4.296 dynes/cm^2.

Finally, the most recent solar model calculations (with further program improvements) were completed at the Naval Research Laboratory in November 1966. There resulted: T_c = 1813.7 eV, ρ_c = 30.0 g/cc, M = 1.990^{33}g, R = 6.96^{10} cm, and L = 3.90^{33} ergs/sec. The most remarkable feature of this last model is that it not only yielded P_e vs T in the photosphere in very good agreement with the Utrecht 1964 model of the solar photosphere (28) but also yielded densities that lead to excellent correlations of screened

Coulomb solutions of the Schrödinger equation (29-32) with the drop in intensity of hydrogen lines. The initial results for this unsolved problem were reported by Rouse (33).

The photospheric points are shown in Table 9, with additional calculations shown in Table 10. Note that the third photospheric point — near the Utrecht minimum temperature — indicates that a weak H_{17} line would be the maximum Balmer line observed in absorption. The analysis of Moore, Minnaert, and Houtgast (34) confirms this.

Table 9

The Effective Maximum Bound State n^* and the Last Discrete Level n_m at Three Points in the Solar Photosphere and One Point in the Chromosphere. The Photospheric Points are from a Solar Model (R) and are Compared with the Utrecht 1964 Model of the Photosphere (U). The Radius of the Mean Atomic Volume is r_o, with $n^{*2} = 0.59\, Zr_o/a_o$, and $n_m^2 = Zr_o/a_o$.

h (km)	T (°K)	P_e (dynes/cm^2)	ρ (g/cm^3)	r_o (cm)	$n^*(r_o)$	$n_m(r_o)$
R —	5775	13.2	2.66^{-7}	1.28^{-6}	12	16
U 46	5735	13.3	—	—	—	—
R —	5177	3.65	2.24^{-7}	1.35^{-6}	12	16
U 104	5100	3.36	—	—	—	—
R —	4577	1.05	1.85^{-7}	1.44^{-6}	13	16.5‡
U 173	4590†	1.18	—	—	—	—
R —	5150	0.11	1.0^{-9}	8.22^{-6}	30	39
U 635	5125	0.14	—	—	—	—

†The minimum temperature in the Utrecht model is 4500 ± 50°K at h = 197 km.
‡Model predicts H_{17} as the maximum Balmer Line in absorption. In the NBS Monograph #61, dated December 1966 entitled "The Solar Spectrum 2935 Å to 8770 Å," by C. E. Moore, M. G. J. Minnaert and J. Houtgast, the authors conclude that of the Balmer lines of hydrogen, "... H_{15}, H_{16}, and H_{17} are measurable. The line H_{18} is certainly not seen; ... ."

Table 10

The Effective Maximum Bound State Calculated with the Debye Radius DR and the Last Discrete Level n_m Calculated with the Inglis-Teller Formula $n_m(I-T)$ and with Mohler's Empirical Formula $n_m(M)$. Three Points of Table 1 are Shown Here, Where $n^*(r_o)$ is Repeated.

$n^*(r_o)$	DR§ (cm)	$n^*(DR)$	N_e (electrons/cc)	$n_m(IT)$†	$n_m(M)$‡
12	9.04^{-5}	101	1.65^{13}	22	20
12	1.50^{-4}	130	5.11^{12}	26	24
30	9.03^{-4}	318	1.51^{11}	41	39

†Inglis-Teller formula [Ap. J. 90:439 (1939)]; 7.5 log n_m = 23.26 - log N_e.
‡Mohler's formula [Ap. J. 90:429 (1939)]; 7.5 log n_m = 23.06 - log N_e.
§DR taken from Nature 212:803 (1966).

SUMMARY AND CONCLUSIONS

An ionization equilibrium equation of state has been used in the calculation of stellar structure through an explicit differencing scheme. Applied to the sun, this method has given the first known continuous calculation of the sun's mass, radius, luminosity, and structure of the photosphere interior to the 5800°K radius. To calculate the radius it was necessary to use as a parameter a helium abundance that varied as a function of the relative solar mass (or, in effect, the relative radius). In addition, central densities considerably lower than recently published values had to be assumed. Interior conditions were also shown to be dependent on the photospheric H/He ratio. Solutions with a H/He ratio in the photosphere of 20 indicate a central temperature T_c between 1650 and 1700 eV ($\approx 19.5 \times 10^6$ °K) and a central density ρ_c near 36 g/cc. Solutions with a H/He ratio in the photosphere of 5.55 indicate $T_c \approx 1800$ eV ($\approx 21 \times 10^6$ °K) and $\rho_c \approx 30$ g/cc. A significantly different abundance of carbon-nitrogen in the core would lead to solutions with different values of T_c and ρ_c.

A solution with $T_c \approx 1000$ eV and $\rho_c \approx 42$ g/cc would require energy generation through the proton cycle more than an order of magnitude greater than that given by present formulas.

The calculated mass and radius were shown to depend significantly on the high-density formulation of the equation of state. The effect would have been much greater had high central densities led to a more complete solution.

Stability criteria based on changes in the effective gamma and the mean molecular weight different from the changes along the equilibrium profile were shown to be compatible with perturbations that could lead to granulation, prominences, or the ejection of matter hot enough to help account for the high temperature and irregular nature of the chromosphere.

The ability to calculate temperatures, electron pressures, and densities (with the associated drop in intensity of hydrogen lines) in photosphere models, with solar model calculations that begin at the center, has been demonstrated. Determination of a good H/He ratio in the photosphere and the electron pressure and temperature at an observable point (or points) in the photosphere would establish boundary conditions that must be satisfied by the solution of the solar interior.

In conclusion, we have considered the equilibrium profile of an inhomogeneous, self-gravitating sphere of one solar mass, radius, and luminosity. In future work, approximations to convective motion and rotation should be considered.

ACKNOWLEDGMENTS

This review was written in Washington, D.C., while the author was a Research Associate with the E. O. Hulburt Center for Space Research, Naval Research Laboratory. The work was supported by the Office of Naval Research and the National Science Foundation.

I thank the staff of the E. O. Hulburt Center for the encouragement given for the present approach to the solar structure problem. In particular, I valued the discussions with Dr. Talbot Chubb.

REFERENCES

1. Rouse, C.A., Ap. J. 135:599 (1962a)

2. Rouse, C.A., Ap. J. 136:636 (1962b)

3. Rouse, C.A., Ap. J. 137:1286 (1963a)

4. Chandrasekhar, S., "An Introduction to the Study of Stellar Structure, New York: Dover, 1957 (first published 1939)

5. Kuiper, G.P., editor, "The Sun," Chicago:University of Chicago Press, 1953

6. Schwarzschild, M., "Structure and Evolution of the Stars," Princeton, New Jersey: Princeton University Press, 1958

7. Aller, L.H., and McLaughlin, D.B., editors, "Stellar Structure," Chicago and London: Univ. of Chicago Press, 1965

8. Motz, L., and Duveen, A., "Essentials of Astronomy," Belmont, California:Wadsworth, Inc., 1966

9. Rouse, C.A., "Calculation of Stellar Structure Using an Ionization Equilibrium Equation of State," UCRL 7820-T, Apr. 1964; UCRL 7820 Rev. I, July 20, 1964; UCRL 7820 Rev. I, Supplement, Jan. 7, 1965 (1964b)

10. Rouse, C.A., Ap. J. 134:435 (1961)

11. Rouse, C.A., Ap. J. 136:665 (1962c)

12. Rouse, C.A., Proc. 6th Int. Conf. on Ionization Phenomena in Gases, Paris, Vol. I, p. 225, 1963b

13. Rouse, C.A., Ap. J., 139:339 (1964a)

14. Goldberg, L., Müller, E.A., and Aller, L.H., Astrophys. J. Suppl. 5(No. 45) (1960)

15. Fowler, R.H., "Statistical Mechanics," 2nd ed., Cambridge:Cambridge University Press, 1936

16. Hilsenrath, J., Green, M.S., and Beckett, C.W., "Internal Energy of Highly Ionized Gases," in "IXth International Astronautical Congress, Amsterdam 1958," Proceedings, Wien:Springer-Verlag, Vol. I, pp. 120-136, 1959

17. Woolley, R. v. d. R., and Stibbs, D.W.N., "The Outer Layers of a Star," Oxford: Clarendon Press, 1953

18. Brush, S.G., "Theories of the Equation of State of Matter at High Pressures and Temperatures," in "Progress In High Temperature Physics and Chemistry," Vol. 1, C.A. Rouse, editor, London, New York:Pergamon, 1967

19. Chandrasekhar, S., and Münch, G., Astrophys. J. 104:446 (1946)

20. Cox, A.N., "Stellar Absorption Coefficients and Opacities," in "Stellar Structure," A.H. Aller and D.B. McLaughlin, editors, Chicago: Univ. of Chicago Press, 1965

21. Armstrong, B.H., Johnston, R.R., Kelly, P.S., DeWitt, H.E., and Brush, S.G., "Opacity of High Temperature Air," in "Progress In High Temperature Physics and Chemistry," Vol. 1, C.A. Rouse, editor, London and New York: Pergamon, 1967

22. Reeves, H., "Stellar Energy Sources," in "Stellar Structure," L.H. Aller and D.B. McLaughlin, editors, Chicago: Univ. of Chicago Press, 1965

23. Allen, C.W., "Astrophysical Quantities," London: Athlone Press, 1955; Op. cit., 2nd ed., 1963

24. Leighton, R.B., "Annual Review of Astronomy and Astrophysics," L. Goldberg, editor, Annual Reviews, Inc., Palo Alto, California, Vol. 1, 1963

25. Slater, J.C., "Quantum Theory of Atomic Structure," New York: McGraw-Hill, Vol. 1, Table 8-3, 1960

26. Aller, L.H., "Astrophysics - The Atmospheres of the Sun and Stars," New York: Ronald Press, 2nd ed., 1963

27. Rouse, C.A., A. P. S. Bull. 10:14 (1965)

28. Heintze, J.R.W., Hubenet, H., and de Jager, C., Bull. Astronomical Institutes, Netherlands, 17:442 (1964)

29. Rouse, C.A., "Accurate and Stable Numerical Solutions to the Schrödinger Equation," Feb. 7, 1966; APS Bull. 11:356 (1966); NRL Report 6558; J. of Math. and Phys. 46:63 (1967)

30. Rouse, C.A., "A Finite Electronic Partition Function from Screened Coulomb Interactions," June 21, 1966; revised Jan. 4, 1967 as NRL Report 6556; revised Feb. 24, 1967; Phys. Rev. (to be published)

31. Rouse, C.A., "Screened Coulomb Solutions of the Schrödinger Equation," June 21, 1966; revised Feb. 14, 1967 for the Physical Review 159:41 (1967)

32. Rouse, C.A., "The Screened Coulomb Electronic Partition Function," Mar. 8, 1967, for the VIII Conf. on Phenomena in Ionized Gases, Vienna, Austria

33. Rouse, C.A., Nature 212:803 (1966c); APS Bull. 12:32 (1967)

34. Moore, C.E., Minnaert, M.G.J., and Houtgast, J., "The Solar Spectrum 2935 Å to 8770 Å," NBS Monograph 61, Dec. 1966

This page intentionally left blank.

Security Classification

DOCUMENT CONTROL DATA - R & D

(Security classification of title, body of abstract and indexing annotation must be entered when the overall report is classified)

1. ORIGINATING ACTIVITY *(Corporate author)* Naval Research Laboratory Washington, D.C. 20390	2a. REPORT SECURITY CLASSIFICATION Unclassified 2b. GROUP

3. REPORT TITLE

CALCULATIONS OF STELLAR STRUCTURE

4. DESCRIPTIVE NOTES *(Type of report and inclusive dates)* A survey report of the work accomplished on the problem; work on other phases continues.

5. AUTHOR(S) *(First name, middle initial, last name)*

Carl A. Rouse

6. REPORT DATE September 18, 1967	7a. TOTAL NO. OF PAGES 28	7b. NO. OF REFS 34
8a. CONTRACT OR GRANT NO. NRL Problem A01-02 b. PROJECT NO. Project RR 004-02-42-5300 c. d.	9a. ORIGINATOR'S REPORT NUMBER(S) NRL Report 6580 9b. OTHER REPORT NO(S) *(Any other numbers that may be assigned this report)*	

10. DISTRIBUTION STATEMENT

Distribution of this document is unlimited.

11. SUPPLEMENTARY NOTES	12. SPONSORING MILITARY ACTIVITY Department of the Navy (Office of Naval Research), Washington, D.C. 20360

13. ABSTRACT

Calculations of the author's solar model, reported at the New York APS meeting, Jan. 1965, were continued at the Naval Research Laboratory as part of a research program undertaken as an E. O. Hulburt Research Appointee. Of particular significance is that due to the increased mathematical and physical accuracies introduced at NRL, the resulting photospheric densities lead to mean atomic volumes in excellent agreement with those needed to explain the drop in intensity of photospheric hydrogen lines through screening. The solar model itself is the first known continuous calculation — from the center through the photosphere — of the sun's mass, radius, and luminosity. The resulting model, incidentally, yields values of electron pressure and temperature in the photosphere in good agreement with the currently accepted photospheric values.

The present report reviews the method and the progress leading to the present equilibrium model with the inclusion of results obtained as part of current NRL research. This review is to be published in Vol. 2 of "Progress in High Temperature Physics and Chemistry," of which the author is the editor for Pergamon Press.

DD FORM 1 NOV 65 1473 (PAGE 1)

S/N 0101-807-6801

Security Classification

Security Classification

14. KEY WORDS	LINK A ROLE	LINK A WT	LINK B ROLE	LINK B WT	LINK C ROLE	LINK C WT
Stellar structure						
Sun						
Helium abundance						
Radius						
Mass						
Central density						
Opacity						
Luminosity						
Energy generation						
Ionization equilibrium equation of state						
Adiabatic change						
Radiative gradient						
Convective gradient						
Photosphere						
Solar granulation						

DD FORM 1 NOV 65 1473 (BACK)
(PAGE 2)

GPO 931-088

Security Classification